J. Phys. Chem. 1983, 87, 3769-3774

chlorophylls concentrated on lipid membranes in chloroplasts.

Acknowledgment. We are grateful to Professor Keitaro Yoshihara and Dr. Nobuaki Nakashima of the Institute for Molecular Science, for the fluorescence decay measurements with a picosecond laser. We are grateful to Professor Shoichi Ikeda, Nagoya University, for the measurement of the cmc of PGME and helpful discussions, to Dr. Yoshihumi Kusumoto, Kagoshima University, for helpful discussions, and to Messrs. Shigeki Takeo, Shigeo Tanahashi, and Yasuo Suzuki for their assistance in the experiments. This work is partly supported by a Grant-in-Aid for Scientific Research (447006) of the Ministry of Education, Science, and Culture of Japan.

Appendix

Probability Function for the Random Distribution of the Donor and Acceptor on a Sphere. The probability $\rho(R)\,dR$ that an acceptor is found at the distance between R and $R + dR$ from the donor is calculated for the case that the donor and the acceptor are distributed randomly on a sphere of radius r. (See Figure 15.)

The probability is given to be

$$\rho(R)\,dR = \beta\int_{\phi=0}^{2\pi} dS = \beta\int_{\phi=0}^{2\pi} r^2 \sin\theta\,d\theta\,d\phi = 2\pi\beta r^2 \sin\theta\,d\theta \qquad \text{(A-1)}$$

where β is a constant. From the law of cosines

$$(R + dR)^2 = 2r^2 - 2r^2 \cos(\theta + d\theta) \qquad \text{(A-2)}$$

$$R^2 = 2r^2 - 2r^2 \cos\theta \qquad \text{(A-3)}$$

we obtain

$$R\,dR = r^2 \sin\theta\,d\theta \qquad \text{(A-4)}$$

On substituting eq A-4 into eq A-1 we have

$$\rho(R)\,dR = 2\pi\beta R\,dR \qquad \text{(A-5)}$$

Finally, by putting $2\pi\beta = \alpha$, we obtain

$$\rho(R) = 2\pi\beta R = \alpha R \qquad \text{(A-6)}$$

Registry No. Rhodamine 6G, 989-38-8; pinacyanol, 605-91-4; sodium dodecyl sulfate, 151-21-3.

Oscillations in the Bromate–Bromide–Cerous System. The Simplest Chemical Oscillator

K. Bar-Eli*

Department of Chemistry, Tel-Aviv University, 69978 Ramat Aviv, Israel

and W. Geiseler

Institut fur Technische Chemie, Technische Universitat, West Berlin, D-1000 West Berlin 12, FRG *(Received: October 25, 1982; In Final Form: April 29, 1983)*

The bistability of the cerium–bromate–bromide system in an open-flow (CSTR) system was investigated near the critical point. Near this critical point Hopf's bifurcation occurs, causing stable states to become unstable. Domains of single or three unstable steady states occur, with possible oscillations around them. A good agreement is obtained between the calculated and experimental oscillation domains on the various subspaces of constraints. This oscillator is the simplest chemical oscillator fully understood in terms of elementary reactions.

Introduction

The investigated system of bromate, bromide, and cerium ions in a continuous stirred tank reactor (CSTR) was shown earlier[1] to exist, under certain constraints, in more than one steady state. Transitions between these steady states show regular hysteresis phenomena. Computations according to the accepted Noyes–Field–Thompson (NFT) mechanism[2] and experimental[3-5] data are in very good agreement, thus confirming the mechanism in general and the rate constants used in particular.

Recently, it was predicted[6] that, under certain conditions, the system might show oscillations in addition to the well-established bistability and hysteresis. These predictions were rather unexpected since the system does not contain malonic or bromomalonic acid, which were thought to provide the necessary pathway of ceric ion reduction after it had been oxidized by the $BrO_2\cdot$ radical, derived from the bromate ion. The chemical arguments which are the basis of the Field–Körös–Noyes (FKN) mechanism[7] of the oscillating Belousov–Zhabotinskii (BZ) reaction[8] are

---

(1) W. Geiseler and H. Föllner, *Biophys. Chem.*, **6**, 107 (1977).

(2) R. M. Noyes, R. J. Field, and R. C. Thompson, *J. Am. Chem. Soc.*, **93**, 7315 (1971).

(3) K. Bar-Eli and R. M. Noyes, *J. Phys. Chem.*, **81**, 1988 (1977).

(4) K. Bar-Eli and R. M. Noyes, *J. Phys. Chem.*, **82**, 1352 (1978).

(5) W. Geiseler and K. Bar-Eli, *J. Phys. Chem.*, **85**, 908 (1981).

(6) K. Bar-Eli in "Nonlinear Phenomena in Chemical Dynamics", Vol. 12, C. Vidal and A. Pacault, Eds., Springer Series in Synergetics, Springer-Verlag, West Berlin, 1981, pp 228–39.

(7) (a) R. J. Field, E. Körös, and R. M. Noyes, *J. Am. Chem. Soc.*, **94**, 8649 (1972); (b) R. J. Field and R. M. Noyes, *J. Chem. Phys.*, **60**, 1877 (1974).

(8) (a) B. P. Belousov, *Sb. Ref. Radiats. Med. 1958, Medgiz. Moscow*, 145 (1959); (b) A. M. Zhabotinskii, *Dokl. Akad. Nauk USSR*, **157**, 392 (1969); (c) A. M. Zhabotinskii, *Biofizica*, **9**, 306 (1964); (d) A. N. Zaikin and A. M. Zhabotinskii, *Nature (London)*, **225**, 535 (1970).

(9) M. Orban, F. De Kepper, and I. R. Epstein, *J. Am. Chem. Soc.*, **104**, 2657 (1962).

(10) (a) W. Geiseler, *Ber. Bunsenges. Phys. Chem.*, **86**, 721 (1982); (b) W. Geiseler, *J. Phys. Chem.*, **86**, 4394 (1982).

(11) (a) J. H. Woodson and H. A. Liebhafsky, *Anal. Chem.*, 41, 1894 (1969); (b) N. Ganapathisubramanian and R. M. Noyes, *J. Phys. Chem.*, **86**, 3217 (1982).

(12) J. A. Dean, "Chemical Separation Methods", Van Nostrand, Princeton, NJ, 1969.

(13) L. R. Snyder, *Chromatog. Rev.*, **7**, 1 (1965).

(14) H. Lachmann, private communication.

(15) W. M. Latimer, "Oxidation Potentials", 2nd ed., Prentice-Hall, New York, 1952.

(16) S. Barkin, M. Bixon, R. M. Noyes, and K. Bar-Eli, *Int. J. Chem. Kinet.*, **11**, 841 (1977).

(17) (a) C. W. Gear, "Numerical Initial Value Problems in Ordinary Differential Equations", Prentice-Hall, Englewood Cliffs, NJ, 1971, pp 209–29; (b) A. C. Hindmarsh, "Gear: Ordinary Differential Equations Systems Solver", VCID 2001, rev 3, Dec 1974.

0022-3654/83/2087-3769$01.50/0

given in detail elsewhere.[20] The verifications of the predicted oscillations, in two different laboratories,[9,10] show that one cannot always rely on simple chemical intuition and arguments and the latter must always be supported and supplemented by detailed calculations.

In this paper we want to recapitulate the arguments and calculations which led us to believe that the present simple system will oscillate, compare the computed and experimental data, and also provide some new and unpublished data.

It is important to note that this system is the simplest one which shows bistability and oscillations and for which the mechanism is known in complete detail in terms of elementary reactions.

Experimental Section

The experimental device consists of an isothermal CSTR which is fed by a peristaltic pump with sulfuric acid solutions of $KBrO_3$, KBr, and $Ce_2(SO_4)_3$ via separate inlet tubes. The behavior of the CSTR is followed by simultaneously recording the absorbance of ceric ions and measuring the bromide concentration by means of a bromide-sensitive electrode. At low bromide concentrations ($[Br^-] < 10^{-6}$ M) this electrode did not follow the Nernst equation[11] but reliably indicated the transition points and oscillations that we were interested in. More details are given elsewhere.[5]

The linear gradient device used for slowly changing $[Br^-]_0$ between suitably chosen $[Br^-]_{0,max}$ and $[Br^-]_{0,min}$ consists of two communicating cylinders of equal cross section, namely, the reservoir and the mixing chamber. From the latter $[Br^-]_0$ is withdrawn at a constant feed rate. The fundamental aspects of such devices have been described in detail by Dean[12] and Snyder.[13] The efficiency of our device has been tested with water (mixing chamber) and an aqueous solution of ferroin (1,10-phenanthroline-iron(II) sulfate) the absorbance of which was measured spectrophotometrically at $\lambda = 509$ nm in a flow-through cuvette. The linearly increasing ferroin absorbance[10] indicates a linear relationship between concentration in the flow and time. A negative gradient could also be obtained by reversing the initial contents of the vessels.

In order to avoid random searching for oscillations, we first measured the region of steady-state multiplicity and determined the critical point beyond which the region of oscillations could be expected. Beyond the critical point, we applied the linear gradient method for finding and measuring the oscillation region. In our experiments we changed $[Br^-]_0$ and kept other constraints constant. Thus, the CSTR followed a line parallel to the $[Br^-]_0$ axis of Figure 3. The same points of onset and end of oscillations were obtained, regardless of whether the $[Br^-]_0$ gradient was positive or negative, i.e., whether $[Br^-]_0$ increases or decreases with time.

A series of such measurements with stepwise varied $[BrO_3^-]_0$, or other species, or flow rate yielded the points given in Figures 3–6.

Sustained oscillations at points inside the oscillation domain were obtained by stopping the gradient and continuing the experiment with constant $[Br^-]_0$. The oscillations persist as long as the fluxes to and from the CSTR are maintained. The purity of chemicals used and the material of reactor walls seem to affect the position and size of the oscillation domain. Oscillations were also obtained when a continuously working pump[14] was used instead of the peristaltic pump, thus proving that the oscillations are not due to the particular experimental device used. The sensitivity of the oscillation to external conditions will be described below.

Calculations and Results

The NFT mechanism is made up of the following seven chemical reactions, the rate constants of which are shown. These rate constants are partly measured,[7a] partly estimated,[15] and slightly corrected to agree better with kinetic data.[16]

$$BrO_3^- + Br^- + 2H^+ \rightleftarrows HBrO_2 + HOBr \qquad (1)$$

$$k_1 = 2.1\ M^{-3}\ s^{-1} \qquad k_{-1} = 1 \times 10^4\ M^{-1}\ s^{-1}$$

$$HBrO_2 + Br^- + H^+ \rightleftarrows 2HOBr \qquad (2)$$

$$k_2 = 2 \times 10^9\ M^{-2}\ s^{-1} \qquad k_{-2} = 5 \times 10^{-5}\ M^{-1}\ s^{-1}$$

$$HOBr + Br^- + H^+ \rightleftarrows Br_2 + H_2O \qquad (3)$$

$$k_3 = 8 \times 10^9\ M^{-2}\ s^{-1} \qquad k_{-3} = 110\ s^{-1}$$

$$BrO_3^- + HBrO_2 + H^+ \rightleftarrows 2BrO_2\cdot + H_2O \qquad (4)$$

$$k_4 = 1 \times 10^4\ M^{-2}\ s^{-1} \qquad k_{-4} = 2 \times 10^7\ M^{-1}\ s^{-1}$$

$$Ce^{3+} + BrO_2\cdot + H^+ \rightleftarrows Ce^{4+} + HBrO_2 \qquad (5)$$

$$k_5 = 6.5 \times 10^5\ M^{-2}\ s^{-1} \qquad k_{-5} = 2.4 \times 10^7\ M^{-1}\ s^{-1}$$

$$Ce^{4+} + BrO_2\cdot + H_2O \rightleftarrows Ce^{3+} + BrO_3^- + 2H^+ \qquad (6)$$

$$k_6 = 9.6\ M^{-1}\ s^{-1} \qquad k_{-6} = 1.3 \times 10^{-4}\ M^{-3}\ s^{-1}$$

$$2HBrO_2 \rightleftarrows BrO_3^- + HOBr + H^+ \qquad (7)$$

$$k_7 = 4 \times 10^7\ M^{-1}\ s^{-1} \qquad k_{-7} = 2.1 \times 10^{-10}\ M^{-2}\ s^{-1}$$

The rate constants are used with the assumption that the concentration of water is constant at unit activity. Including the concentration of water as a variable in the calculations was examined, and the same results were obtained; thus, this extra complication was abandoned.

To the rate equations formed from the seven reactions 1–7, the terms $k_0(C_{0i} - C_i)$ are added, where C_i is the concentration of species i, C_{0i} is the concentration of this species in the feed flow, and k_0 is the ratio between the flow rate $\dot{V}$ and the volume of the reaction vessel V_R. Its reciprocal is sometimes called the "retention time" or "residence time".

The equations thus obtained are

$$dC_i/dt = F_i(C) + k_0(C_{0i} - C_i) \qquad (8)$$

where $F_i(C)$ describes the chemical mass action rates derived from eq 1–7. Equation 8 was solved by Newton's method for a steady state, i.e., for $\dot{C} = 0$, or by the Gear[17] method where oscillations are expected.

The parameters or the external constraints of the system are k_0 and C_{0i}. In our case there are five of them, namely, k_0, $[BrO_3^-]_0$, $[Br^-]_0$, $[Ce^{3+}]_0$, and $[H^+]_0$. The complete description of the system must, therefore, be given in five dimensions. All figures are obviously two-dimensional cross sections of this five-dimensional space, as the other three are kept constant.

The temperature is also an external constraint and the system is, in fact, very sensitive to it, as will be seen below. The temperature influences the system indirectly by changing the various rate constants, each according to a

---

(18) P. De Kepper and K. Bar-Eli, *J. Phys. Chem.*, **87**, 480 (1983).

(19) K. Bar-Eli and W. Geiseler, *J. Phys. Chem.*, **87**, 1352 (1983).

(20) (a) R. J. Field and R. M. Noyes, *Acc. Chem. Res.*, **10**, 214 (1974); (b) J. J. Tyson in "Lecture Notes on Biomathematics", S. A. Levine, Ed., Springer-Verlag, West Berlin, 1976.

(21) (a) J. Boissonade and P. De Kepper, *J. Phys. Chem.*, **84**, 501 (1980); (b) P. De Kepper and J. Boissonade, *J. Chem. Phys.*, **75**, 189 (1981).

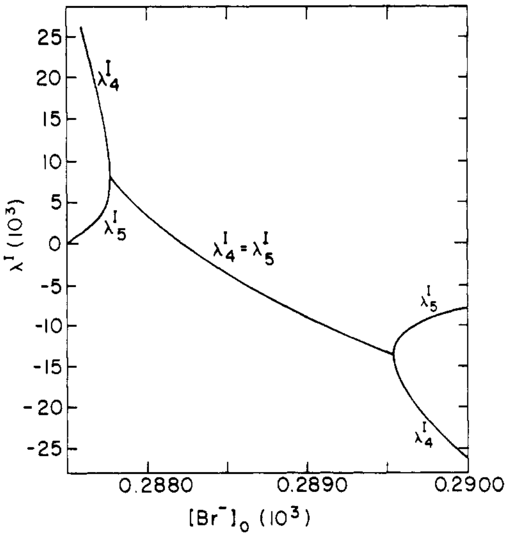

Figure 1. Change of two eigenvalues of SSI which become a conjugate pair vs. $[Br^-]_0$. Only the real part of the pair is shown. Constant constraints: $[BrO_3^-]_0 = 56.405924 \times 10^{-3}$ M, $[Ce^{3+}]_0 = 1.5 \times 10^{-4}$ M, $[H^+]_0 = 1.5$ M, $k_0 = 4. \times 10^{-3}$ s^{-1}. Coalescence of real eigenvalues to conjugate pair at $[Br^-]_0 = 2.8954 \times 10^{-4}$ M and $[Br^-]_0 = 2.8777 \times 10^{-4}$ M. Hopf's bifurcation at $[Br^-]_0 = 2.8821 \times 10^{-4}$ M. $J = \lambda_5 = 0$ at $[Br^-]_0 = 2.87517 \times 10^{-4}$ M.

different, and usually unknown, activation energy.

The effect of changing the various rate constants is dealt with by Geiseler and Bar-Eli.[5,19] Conservation laws and the dependencies of some of the reactions on others reduce the number of independent species from nine to five. The detailed mathematical procedure of handling these dependencies is given elsewhere.[6,18,19]

The solution of eq 8 shows that, in a certain range of constraints, the system can exist in three steady states:[1,3-5] SSI has a relatively high concentration of bromide and low concentration of ceric ions. SSII has a relatively low concentration of bromide and high concentration of ceric ions. This steady state is the one which will go over smoothly to equilibrium as k_0 becomes zero, i.e., when the system is closed. Between these two stable steady states, a third unstable one, SSIII, exists. Being unstable, it cannot, of course, be attained experimentally. The transition between the physically attainable SSI and SSII can be achieved by changing slowly a certain constraint (such as the bromide ion concentration) and tracing a hysteresis cycle,[5] or by introducing a strong perturbation.[10b,19]

As the constraints are changed, a critical point is reached, beyond which a smooth transition between the SS, without hysteresis, will occur. The hysteresis limits were calculated and tested experimentally by Geiseler and Bar-Eli.[5] The comparison between the experimental and calculated data was used by the above authors to obtain accuracy limits for the various rate constants.

The three steady states are characterized by the equations $\dot{C}_i = 0$ where C_i are the concentrations of the various species in the reaction cell. The Jacobian matrix $\partial\dot{C}_i/\partial C_j$ has eigenvalues with negative real parts for SSI and SSII, while SSIII must have at least one eigenvalue with a positive real part.

When the system is far away from the critical point, all its eigenvalues (λ) are real and the Jacobian $J = \prod_i \lambda_i$ is negative for SSI and SSII and positive for SSIII. At the hysteresis limits, i.e., at the transitions from SSI (or SSII) to SSIII, one of the eigenvalues and J become zero and the Jacobian matrix will become singular. As the system approaches the critical point, two real eigenvalues coincide to become a conjugate pair, as shown in Figure 1, for the pair belonging to SSI. A similar phenomenon happens for SSII. When the real part of two such conjugate eigenvalues changes its sign, the sign of the Jacobian determinant remains negative as before. The Jacobian does not become zero at this point since the imaginary part will contribute its share. In other words, the Jacobian matrix remains regular at this point. When the real part of such a conjugate pair changes its sign, i.e., a Hopf bifurcation[23] occurs, the stability of the SS is lost. In Figure 2 the region near the critical point in $[Br^-]_0$–$[BrO_3^-]_0$ subspace is shown in detail.

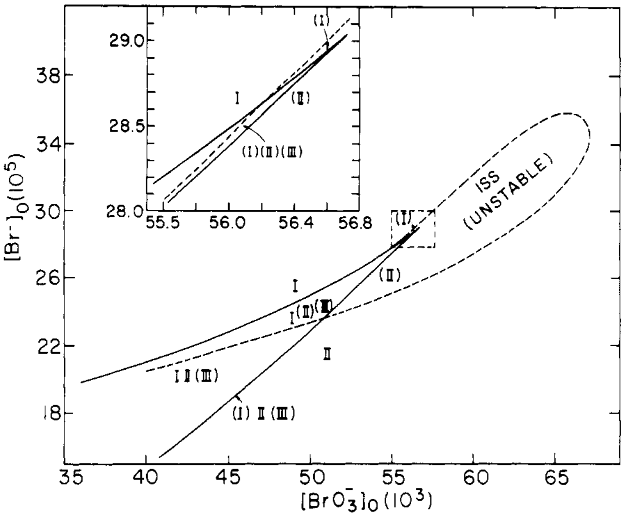

Figure 2. $[Br^-]_0$–$[BrO_3^-]_0$ calculated subspace of constraints near the critical point which occurs at $[BrO_3^-]_0 = 56.7283 \times 10^{-3}$ M, $[Br^-]_0 = 29.037 \times 10^{-5}$ M. Constant constraints: $[Ce^{3+}]_0 = 1.5 \times 10^{-4}$ M, $[H^+]_0 = 1.5$ M, $k_0 = 4 \times 10^{-3}$ s^{-1}. When the symbol of the SS is shown in parentheses, the SS is unstable. Solid line: bistability limits. Dashed line: Hopf's bifurcation.

The Hopf bifurcation points are marked by a dashed line, while the bistability limits are marked by a solid line. The dashed line is seen to make a loop around the critical point, thus creating eight different domains as follows: (1) single stable SSI; (2) single unstable SSI; (3) single stable SSII; (4) single unstable SSII; (5) coexistence of stable SSI and SSII; (6) coexistence of stable SSI and unstable SSII; (7) coexistence of unstable SSI and stable SSII; (8) coexistence of SSI and SSII, both unstable. Wherever SSI and SSII coexist, there will always be an unstable SSIII. Domains 1 and 3 and 2 and 4 extend beyond the critical point where the names I and II lose their meaning since a smooth transition occurs between them. In domains 2, 4, and 8, enclosed between the loop of the dashed lines in Figure 2, oscillation must occur, since in these domains only one or three unstable SS exist. One cannot tell from the above analysis whether the oscillations will be simple periodic, irregular, or even chaotic. However, in all the examined cases the solutions of the differential equations in these domains gave simple periodic solutions with no complications. In principle, domains 6 and 7, where one unstable SS coexists with a stable one, might also show oscillations. However, all computations show that the system always ends up at the stable SS, whatever the initial conditions are. No oscillations associated with the unstable SS were found. In Figure 3, the oscillation domains in $[Br^-]_0$–$[BrO_3^-]_0$ subspace, for various constant constraints, are shown. Plot E corresponds to the conditions of the calculations of Figure 2. All plots are "open" on their lower left side. At this vicinity where the system approaches the critical point calculations become slow and difficult because the Jacobian approaches zero. The main portion of the oscillation domain, i.e., the domain of a single unstable SS, is, however, shown.

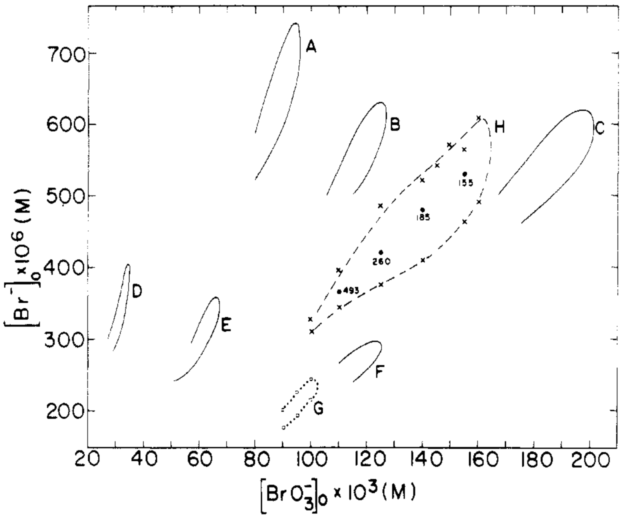

Figure 3. Oscillation domains in $[Br^-]_0$–$[BrO_3^-]_0$ subspace. Constant constraint calculations: (A) $[H^+]_0 = 1.5$ M, $[Ce^{3+}]_0 = 3 \times 10^{-4}$ M, $k_0 = 4 \times 10^{-3}\ s^{-1}$; (B) $[H^+]_0 = 0.75$ M, $[Ce^{3+}]_0 = 3 \times 10^{-4}$ M, $k_0 = 2 \times 10^{-3}\ s^{-1}$; (C) $[H^+]_0 = 0.75$ M, $[Ce^{3+}]_0 = 3 \times 10^{-4}$ M, $k_0 = 5 \times 10^{-3}\ s^{-1}$; (D) $[H^+]_0 = 3.$ M, $[Ce^{3+}]_0 = 1.5 \times 10^{-4}$ M, $k_0 = 4 \times 10^{-3}\ s^{-1}$; (E) $[H^+]_0 = 1.5$ M, $[Ce^{3+}]_0 = 1.5 \times 10^{-4}$ M, $k_0 = 4 \times 10^{-3}\ s^{-1}$; (F) $[H^+]_0 = 0.75$ M, $[Ce^{3+}]_0 = 1.5 \times 10^{-4}$ M, $k_0 = 4 \times 10^{-3}\ s^{-1}$. Experimental: (G) $[H^+]_0 = 0.75$ M, $[Mn^{2+}]_0 = 3 \times 10^{-4}$ M, $k_0 = 5 \times 10^{-3}\ s^{-1}$; (H) $[H^+]_0 = 0.75$ M, $[Ce^{3+}]_0 = 3 \times 10^{-4}$ M, $k_0 = 5 \times 10^{-3}\ s^{-1}$. Dots with numbers: oscillation periods in seconds at the marked points. ×: measured oscillation limits in cerium system. □: measured oscillation limits in manganese system.

Some general trends can be deduced from this figure. As acid concentration is decreased, the oscillation domain is increased and shifts toward higher bromate ion concentrations and slightly lower concentrations of bromide ions. As cerous ion concentration is increased, the domain will increase in size and shift toward higher $[Br^-]_0$ and $[BrO_3^-]_0$ values. The same trend is shown when the flow, i.e., k_0, is increased. It is, therefore, easier to look for the oscillations at low acid concentrations, higher flows, and higher $[Ce^{3+}]_0$.

As seen from these results, the oscillation domain is very sensitive to the other three constraints. In addition to its rather small size, it is quite difficult to detect this domain experimentally. Using the linear gradient device, one can scan a whole range of bromide ion concentration and pinpoint exactly the limits of the oscillation domains.

The experimental oscillation domain for constant $[H^+]_0 = 0.75$ M, $[Ce^{3+}]_0 = 3 \times 10^{-4}$ M, and $k_0 = 5 \times 10^{-3}\ s^{-1}$ is shown and is found to be very near the computed one and of comparable size and shape. The computations show that the oscillation period increases with $[Br^-]_0$ and decreases as $[BrO_3^-]_0$ is increased as shown in Table I. It is seen that a sharp increase in period occurs near the upper left-hand side of the oscillation limit, while a small decrease occurs at the lower right-hand limit. Associated with the increase in period there is also an increase in amplitude. Similar trends are obtained experimentally, as can be seen in Figure 4. The figure shows typical measurements for a bromide-sensitive electrode as the $[Br^-]_0$ is scanned by the linear gradient. At low $[BrO_3^-]_0$, the amplitude and the period are large, while the reverse is true for high $[BrO_3^-]_0$. In each plot the time between peaks, i.e., the period, increases as $[Br^-]_0$ increases. Figure 4 manifests also the increase of amplitude with period. All calculated oscillations and most experimental ones are simple periodic.

Figure 3 also shows the oscillation region of a system that contains manganese ions instead of cerium ones. The oscillation domain is much smaller and located at smaller values of $[BrO_3^-]_0$ and $[Br^-]_0$. This is in complete agreement with the results of Orban et al.[9] and Geiseler[10] which locate the critical point of the manganese system at lower values of $[BrO_3^-]_0$ and $[Br^-]_0$. These changes are due, according to Bar-Eli and Geiseler,[19] to the value of the rate constant of reaction 5 being $k_5 = 1.8 \times 10^5\ M^{-2}\ s^{-1}$ for the manganese case instead of the value given above for the cerium case.

TABLE I: Change of Amplitude and Period with $[BrO_3^-]_0$ and $[Br^-]_0$[a]

$[Br^-]_{max}$/ $[Br^-]_{min}$ of oscillation	τ, s	$10^3 \times [BrO_3^-]_0$, M	$10^6 \times [Br^-]_0$, M
5.1	270 (calcd)	190	600
4.2	182 (calcd)	190	580
3.4	145 (calcd)	190	560
2.7	128 (calcd)	190	540
2.0	122 (calcd)	190	520
6.6	217 (calcd)	180	540
4.1	156 (calcd)	185	540
2.7	128 (calcd)	190	540
1.6	115 (calcd)	195	540
1.7	~156 (exptl)	155	530
2.3	185 (exptl)	140	480
5.7	260 (exptl)	125	420
15	493 (exptl)	110	365

[a] Constant constraints: $[Ce^{3+}]_0 = 3 \times 10^{-4}$ M, $[H^+]_0 = 0.75$ M, $k_0 = 6 \times 10^{-3}\ s^{-1}$.

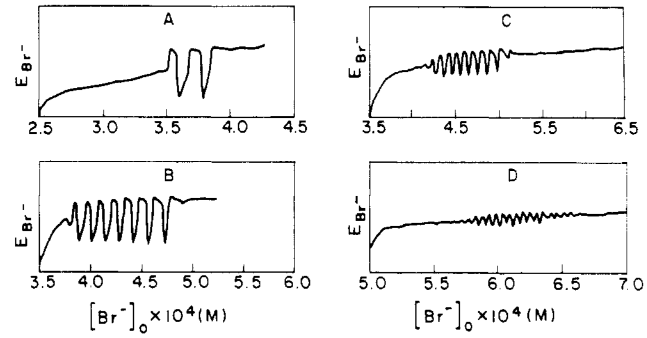

Figure 4. Series of linear gradient experiments, increasing $[Br^-]_0$: (A) $[BrO_3^-]_0 = 0.11$ M; (B) $[BrO_3^-]_0 = 0.125$ M; (C) $[BrO_3^-]_0 = 0.140$ M; (D) $[BrO_3^-]_0 = 0.155$ M. Constant constraints: $[H^+]_0 = 0.75$ M, $[Ce^{3+}]_0 = 3 \times 10^{-4}$ M, $k_0 = 5 \times 10^{-3}\ s^{-1}$.

In Figure 5, the oscillation domain in k_0–$[Br^-]_0$ subspace is shown at two different sets of constraints: one at $[H^+]_0 = 0.75$ M, $[BrO_3^-]_0 = 0.125$ M, and $[Ce^{3+}]_0 = 3 \times 10^{-4}$ M corresponding to the experiments of this work, and the other at $[H^+]_0 = 1.5$ M, $[BrO_3^-]_0 = 0.05$ M, and $[Mn^{2+}]_0 = 1.02 \times 10^{-4}$ M corresponding to the experiments of Orban et al.[9]

The experiments of Orban et al.[9] were done with manganese ions replacing cerium ones as catalysts. So the oscillation region was calculated again for a value of $k_5 = 1.8 \times 10^5\ M^{-2}\ s^{-1}$ and is given in the figure. There is good agreement between the calculated and experimental data for both the cerium and manganese cases.

The calculated data for $k_5 = 1.8 \times 10^5\ M^{-2}\ s^{-1}$ agrees better with the experimental data of Orban et al.,[9] showing, once again, that the choice of the above value for the rate constant of reaction 5 is, indeed, more appropriate for the manganese catalysis.

Figure 6 shows yet another subspace, namely, $[Br^-]_0$–$[Ce^{3+}]_0$. Here, the calculated oscillation domain is rather small compared to the experimental one which extends to much larger values of both $[Ce^{3+}]_0$ and $[Br^-]_0$. An increase of the oscillation amplitude and period is observed with an increase of both $[Br^-]_0$ and $[Ce^{3+}]_0$. These results indicate that, although the given rate constants are

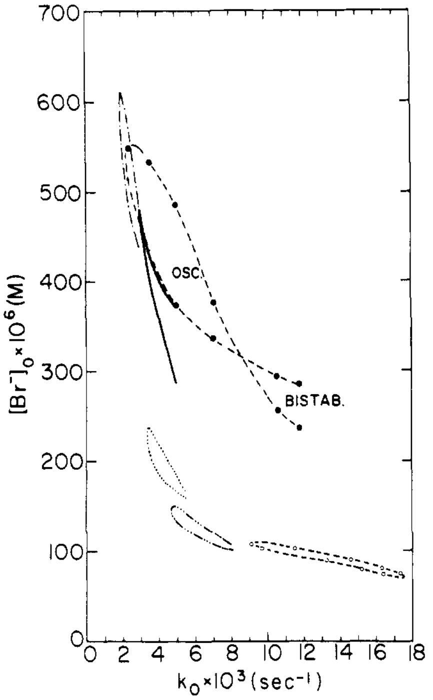

Figure 5. k_0–$[Br^-]_0$ subspace. Constant constraints: $[H^+]_0 = 0.75$ M, $[BrO_3^-]_0 = 0.125$ M, $[Ce^{3+}]_0 = 3 \times 10^{-4}$ M; (●) experimental oscillations and bistability near the critical point, (– • –) calculated oscillations region, (—) calculated bistability region. Constant constraints: $[H^+]_0 = 1.5$ M, $[BrO_3^-]_0 = 0.05$ M, $[Ce^{3+}]_0 = 1.02 \times 10^{-4}$ M; (O) experimental oscillation region of Orban et al.[9] ($[Mn^{2+}]_0 = 1.02 \times 10^{-4}$ M), (•••) calculated oscillation region for $k_5 = 6.5 \times 10^5$ M^{-2} s^{-1}, (–•••–) calculated oscillation region for $k_5 = 1.8 \times 10^5$ M^{-2} s^{-1} (see text).

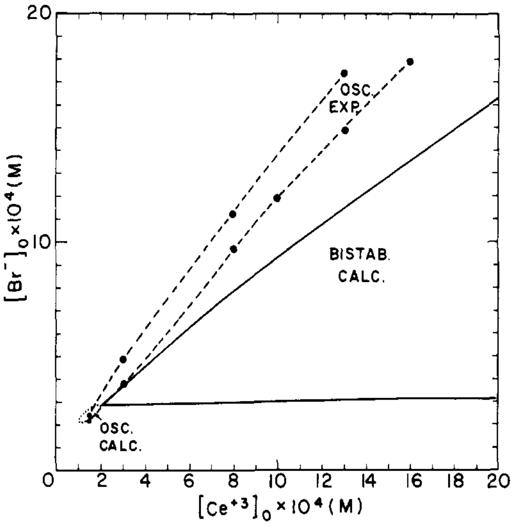

Figure 6. $[Br^-]_0$–$[Ce^{3+}]_0$ subspace. Constant constraints: $[H^+]_0 = 0.75$ M, $[BrO_3^-]_0 = 0.125$ M, $k_0 = 5 \times 10^{-3}$ s^{-1}; (full line) calculated bistability, (dotted line) calculated oscillation region, (●) experimental oscillation limits.

adequate, some adjustments are needed in order to achieve a better agreement with experiment (see Discussion).

Figure 7 shows the dependence of the oscillations on the temperature. As the latter is changed, all the rate constants are changed and thus the limits of the oscillation domain will be changed. A system located at SSI at 21 °C, namely, outside the domain, will move well inside it when the temperature is raised to 22.5 °C, and will move nearly outside again at 26.2 °C. The increase in temperature decreases the period and the amplitude of the oscillations. This is equivalent to moving the plots of Figure 3 upward and to the left with increasing temperature. The last plot in Figure 7 is of very low amplitude, approaching the noise level. The chaotic nature of the oscillations is, therefore, questionable.

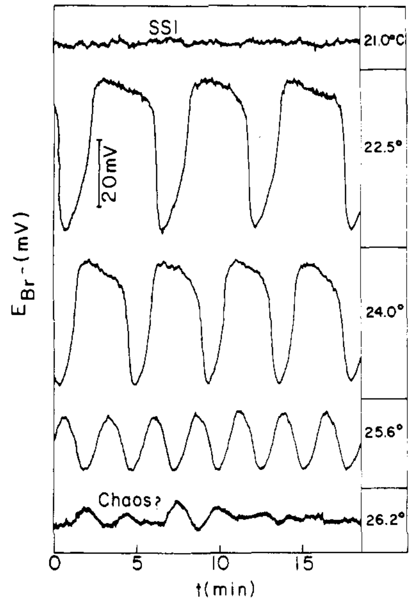

Figure 7. Dependence of sustained oscillations on temperature. Constant constraints: $[BrO_3^-]_0 = 0.14$ M, $[Ce^{3+}]_0 = 3 \times 10^{-4}$ M, $[Br^-]_0 = 4.8 \times 10^{-4}$ M, $[H^+]_0 = 0.75$ M, and $k_0 = 5 \times 10^{-3}$ s^{-1}. Traces of bromine electrode potential with time.

Discussion

A generalized mechanism for bromate-driven oscillation was given by Noyes.[22] The oscillators are divided into five classes and all of them include an organic substrate, such as malonic acid in the BZ reaction. Some classes involve a catalyst, such as cerium ions, while in other classes these ions may be absent. In our system the organic substrate is completely missing. There are only inorganic species and the system oscillates all the same. The chemical processes are, therefore, much simpler and are fully described by the given mechanism that does not fall into any of the categories given by Noyes.

The presented experimental and theoretical data, together with previous evidence, are all in accord with the NFT mechanism. The computations, using the given rate constants, are in good agreement with the experimental data. In order to improve this agreement, some adjustments to the rate constants are necessary. As an example, it was seen above that a slight decrease in the value of k_5 can give a better agreement for manganese catalyst experiments both here and elsewhere.[19]

The changes in the rate constants should be made in such a way as to achieve the best match between the experimental surfaces and the computed ones. These surfaces are the bistability limits (solid lines of Figure 2) and the limits of the oscillation domains, i.e., the surfaces of the Hopf bifurcations (dashed lines in Figure 2). Since both surfaces are implicitly defined, the mathematical problem is of considerable difficulty.

An indication of the difficulty is seen from Figures 4–6. The results of Figures 4 and 5 call for some minor changes in the rate constants in order to obtain a better agreement with experimental data. From Figure 6 it seems, however, that somewhat greater adjustments of the rate constants are necessary to obtain the desired agreement. The two-dimensional cross section of a five-dimensional domain is,

---

[22] R. M. Noyes, *J. Am. Chem. Soc.*, **102**, 4644 (1980).

[23] J. E. Marsden and M. McCraken, "The Hopf Bifurcation and Its Applications", Springer-Verlag, West Berlin, 1976.

therefore, misleading. Only a sound mathematical procedure for making the proper adjustments in the rate constants will be meaningful.

A further difficulty lies in the fact that, at the bistability limits, the Jacobian is zero; i.e., the matrix is singular and has an infinite slope as described elsewhere.[6] This makes all the mathematical procedures in this vicinity more cumbersome. The problem can be slightly reduced by trying to adjust only those rate constants whose values are doubtful or those which are known to be more influential on the position of the surfaces.[5]

A problem of a completely different nature is the generality of this phenomenon. In other words, does every chemical system, which by its nature contains quite a few species and parameters, that shows bistability also oscillate near the critical point? If this is not the case, one should look for the necessary and sufficient conditions to be fulfilled in order for the system to oscillate or to be bistable or both. The existence of oscillations in these situations is also treated by the method of "cross shaped phase diagrams" due to Boissonande and De Kepper.[21] One should note that the oregonator,[20] Field–Körös–Noyes (FKN),[7] and present NFT[2] mechanisms all show oscillations in a region near the critical point.[18,21] Also the chlorite–iodide[24] and Briggs–Rauscher systems[25] show oscillations near the critical point. In the case of the above-mentioned systems, the oscillation domain extends to large portions of the constraints space, while in the present NFT mechanism this portion is rather small and therefore difficult for experimental detection.

Apart from the above disadvantage, this oscillator is the simplest known chemical oscillator, the mechanism of which is completely known in terms of elementary reaction steps. Moreover, unlike the better known BZ oscillator, this one is not influenced by oxygen.[18] It is, therefore, a challenge to find a simpler oscillator.

Registry No. Cerium, 7440-45-1; bromate, 15541-45-4; bromide, 24959-67-9.

---

(24) C. E. Dateo, M. Orban, P. De Kepper, and I. R. Epstein, *J. Am. Chem. Soc.*, **104**, 504 (1982).

(25) (a) T. C. Briggs and W. C. Rauscher, *J. Chem. Educ.*, **50**, 496 (1973); (b) P. De Kepper, Ph.D. Thesis, L'Université de Bordeaux I, France, 1978; (c) P. De Kepper and I. R. Epstein, *J. Am. Chem. Soc.*, **104**, 49 (1982).

Feasibility of Measuring Diffusion Coefficients of Short-Lived Species by Taylor Diffusion

Robert M. Mazo[†]

Department of Chemical Physics, Weizmann Institute of Science, 76100 Rehovot, Israel *(Received: November 2, 1982; In Final Form: February 23, 1983)*

Taylor diffusion in a fluid where the diffusing species is chemically reactive is considered. The question of whether this phenomenon can be used as a tool for the measurement of diffusion coefficients of short-lived species is investigated. It is concluded that such a technique is feasible if the lifetime of the diffusing species is of the order of 1 min or more, in a condensed phase.

Introduction

Almost 30 years ago, Taylor[1] discussed the dispersion of soluble matter in solvent flowing slowly through a tube. One would at first expect that a band of solute in such an experiment would be drawn out by convection into a profile determined by the parabolic velocity profile of the flowing solvent. However, Taylor found that, under certain conditions, the band would move with the mean velocity of the fluid, diffusing about this mean position with an effective diffusion coefficient which can be appreciable larger than the molecular diffusion coefficient. To quote Taylor,[1] "This theoretical conclusion seemed so remarkable that I decided to set up apparatus to see whether the predictions of the analysis could be verified experimentally". In fact, Taylor did verify the predictions by observing the behavior of potassium permanganate (chosen because its intense color facilitated observations) in water and measuring its diffusion coefficient.

The theory of this phenomenon, now called Taylor diffusion, has been further developed by Taylor himself,[2] as well as Aris[3] and others.[4] Furthermore, the effect of heterogeneous chemical reaction of the solute on the walls of the tube has been incorporated into the theory.[5] The purpose of this paper is to propose that Taylor diffusion can be used to measure the diffusion coefficient of relatively short-lived species in solution, and to determine the circumstances under which such a measurement is feasible.

The measurement of the diffusion coefficient of a short-lived species in a condensed phase is extremely difficult. This is because diffusion in condensed phases is quite slow. Hence, particles cannot diffuse very far during their short lifetime, and no measurable concentration profile characteristic of a diffusion experiment is generated. However, since the Taylor diffusion coefficient can be larger by several powers of 10 than the molecular diffusion coefficient, it is possible to magnify the effects of diffusion, using the Taylor phenomenon, so that diffusion coefficients ought to be measurable in favorable cases. The conditions under which Taylor diffusion manifests itself restrict the lifetimes with which one can work to do the order of several tens of seconds. The very interesting region of fractions of a second is still not accessible. Nevertheless, there may well be problems of interest which

---

[†] Permanent address: Department of Chemistry, University of Oregon, Eugene, OR 97403.

(1) Taylor, G. I. *Proc. R. Soc. London, Ser. A* **1953**, *219*, 186.

(2) Taylor, G. I. *Proc. R. Soc. London, Ser. A*, **1954**, *225*, 473.

(3) Aris, R. *Proc. R. Soc. London, Ser. A*, **1956**, *235*, 67.

(4) For a review with references, see: Aris, R. In "Dynamics and Modeling of Reactive Systems"; Stewart, W. E., Harmon, W. H., Conley, C. C., Eds.; Academic Press: New York, 1980.

(5) De Gance, A. E.; Johns, L. E. *Appl. Sci. Res.* **1978**, *34*, 189. This is merely the most recent of a number works of the subject.

0022-3654/83/2087-3774$01.50/0